Crystal structure and magnetic properties of R_5Sn_4 alloys, where R is Tb, Dy, Ho, and Er

X. C. Zhong,[1,2,a)] M. Zou,[2] H. Zhang,[2,4] Z. W. Liu,[1] D. C. Zeng,[1] K. A. Gschneidner, Jr.,[2,3] and V. K. Pecharsky[2,3]
[1]*School of Materials Science and Engineering, South China University of Technology, Guangzhou 510640, China*
[2]*The Ames Laboratory, U.S. Department of Energy, Iowa State University, Ames, Iowa 50011-3020, USA*
[3]*Department of Materials Science and Engineering, Iowa State University, Ames, Iowa 50011-2300, USA*
[4]*State Key Laboratory for Magnetism, Institute of Physics, Chinese Academy of Sciences, Beijing 100190, China*

(Presented 15 November 2010; received 20 September 2010; accepted 10 November 2010; published online 29 March 2011)

Crystal structure and magnetic properties of R_5Sn_4 alloys with R = Tb, Dy, Ho, and Er have been studied. R_5Sn_4, $R_{11}Sn_{10}$, and R_5Sn_3 phases coexist in the annealed alloys and the content of 11:10 and 5:3 phases varies between 9 and 17 wt.%. The R_5Sn_4 major phase has Sm_5Ge_4-type orthorhombic structure with space group *Pnma*. Tb_5Sn_4 has a complex magnetic structure, spin re-orientation and ferrimagnetic-paramagnetic phase transitions occur at ~54 and ~84 K, respectively. For Dy_5Sn_4, Ho_5Sn_4, and Er_5Sn_4, the antiferromagnetic-paramagnetic phase transitions occur at about 22, 15, and 8 K, respectively. The magnetic entropy changes ($-\Delta S_M$) of all alloys are negative at low temperature and changes to positive at higher temperatures, which could be attributed to the change of magnetic states. © *2011 American Institute of Physics*. [doi:10.1063/1.3549562]

The discovery of the giant magnetocaloric effect in $Gd_5Si_2Ge_2$ compound[1] has renewed the interest in rare-earth/Si-group alloys[2–5] in search for materials suitable for magnetic refrigerants. However, information on the physics and chemistry of R_5T_4 phases (T = Sn and Pb, and R = lanthanides except Gd) is still lacking.[6] Bulanova *et al.*[7] assessed the Ho-Sn binary phase diagram and showed existence of Ho_5Sn_4 and Ho_4Sn_5 compounds. They suggested that the Ho_5Sn_4 compound could be formed by the peritectic reaction $L + Ho_5Sn_3 \leftrightarrow Ho_5Sn_4$ at 1720 ± 13 °C. Unfortunately, until now the existence of the compound Ho_5Sn_4 has not been confirmed. Detecting Ho_5Sn_4 phase by x-ray diffraction has not been successful because of the poor quality of the diffraction patterns in the intermediate range of compositions in the system.[7] As for Er-Sn phase diagram,[8] no Er_5Sn_4 phase was reported; but a critical assessment from the available thermodynamic data of binary compounds of lanthanides and group IV elements suggested that both Ho_5Sn_4 and Er_5Sn_4 phases could exist.[9] This theoretical prediction calls for experimental verification. Here we report an experimental study of the crystal structure and magnetic properties of R_5Sn_4 alloys with R = Tb, Dy, Ho, and Er.

The R_5Sn_4 (R = Tb, Dy, Ho and Er) samples were prepared by arc-melting of constituent metals. 3 wt.% excess of Dy, Ho, and Er were added during sample preparation. The purity of Tb, Dy, Ho, Er and Sn was >99.99 wt.%. The ingots were arc melted several times to ensure homogeneity. The as-cast samples were annealed in a vacuum furnace at 1300 °C for 24 h. Powder x-ray diffraction (XRD) data were collected by using an X'Pert PRO diffractometer with Cu $K\alpha_1$ radiation and analyzed by the Rietveld method using Rietica software.

The temperature (T) and magnetic field (H) dependencies of magnetization (M) were measured in a commercial superconducting quantum interference device magnetometer MPMS-XL (Quantum Design Inc). The ac magnetic susceptibility χ_{ac} was measured with magnetic field amplitude of 2.5 Oe and frequency of 125 Hz. The isothermal magnetic entropy change, ΔS_M, was calculated from the isothermal dc magnetization data using the Maxwell equation.[10]

The XRD refinement results of the phase contents in the as-cast and annealed R_5Sn_4 (R = Tb, Dy, Ho, and Er) alloys are listed in Table I. The contents of 5:4 phases increase after annealing, especially in the Ho_5Sn_4 and Er_5Sn_4 alloys. The total amount of 11:10 and 5:3 phases varies between 9 and

TABLE I. The phase composition of the as-cast and annealed R_5Sn_4 alloys.

	Phase content (wt.%)	
Alloy	As-cast	Annealed-1300°/24 h
Tb_5Sn_4	Tb_5Sn_4—82.3	Tb_5Sn_4—90.88
	$Tb_{11}Sn_{10}$—11.97	$Tb_{11}Sn_{10}$—7.34
	Tb_5Sn_3—5.74	Tb_5Sn_3—1.78
Dy_5Sn_4	Dy_5Sn_4—77.22	Dy_5Sn_4—82.22
	$Dy_{11}Sn_{10}$—13.36	$Dy_{11}Sn_{10}$—10.28
	Dy_5Sn_3—9.43	Dy_5Sn_3—7.50
Ho_5Sn_4	Ho_5Sn_4—63.89	Ho_5Sn_4—83.54
	$Ho_{11}Sn_{10}$—19.67	$Ho_{11}Sn_{10}$—7.10
	Ho_5Sn_3—16.44	Ho_5Sn_3—9.36
Er_5Sn_4	Er_5Sn_4—64.93	Er_5Sn_4—88.45
	$Er_{11}Sn_{10}$—14.49	$Er_{11}Sn_{10}$—0.87
	Er_5Sn_3—20.58	Er_5Sn_3—11.68

[a)]Electronic mail: xczhong@scut.edu.cn.

TABLE II. Lattice parameters and unit cell volumes of the R_5Sn_4 phases with the orthorhombic Sm_5Ge_4-type structure.

Alloy	Lattice parameters				Space group	Remark
	a (Å)	*b* (Å)	*c* (Å)	*V* (Å^3)		
Tb_5Sn_4	8.004	15.4180	8.1390	1004.40	Pnma	Ref. [11]
	8.0086(3)	15.4369(7)	8.1390(4)	1006.2084(5)		This work
Dy_5Sn_4	7.9600	15.3600	8.1100	991.570	Pnma	Ref. [12]
	7.9865(5)	15.3693(9)	8.0930(5)	993.3749(1)		This work
Ho_5Sn_4	7.9628(2)	15.3001(4)	8.0534(2)	981.1631(8)	Pnma	This work
Er_5Sn_4	7.9366(1)	15.2330(3)	8.0140(2)	968.9095(4)	Pnma	This work

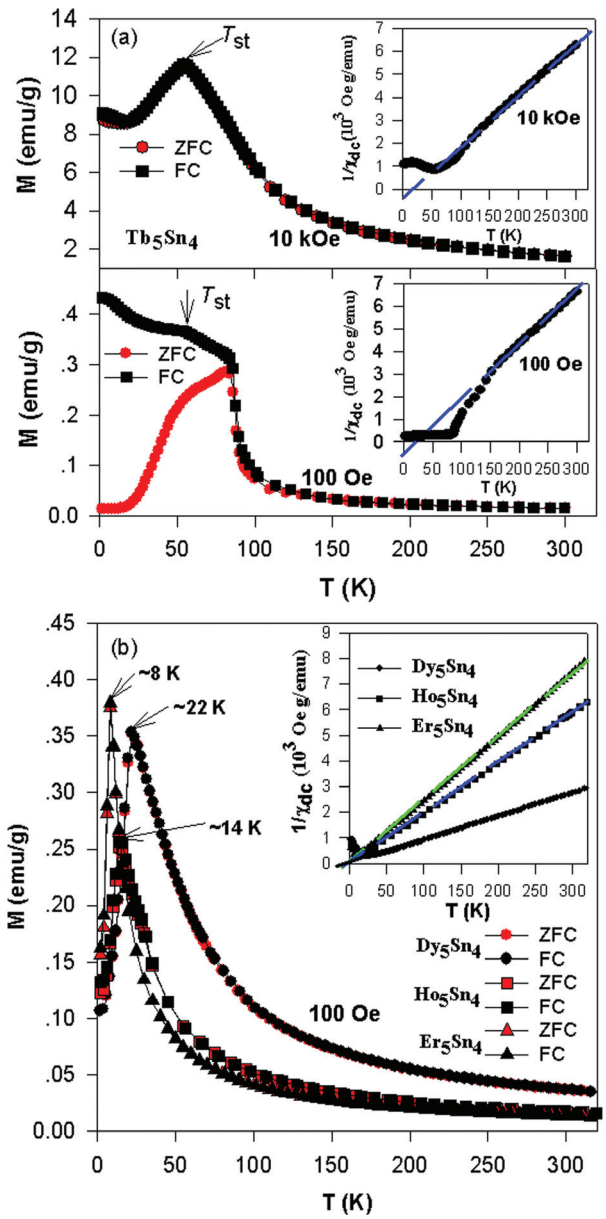

FIG. 1. (Color online) Temperature dependencies of magnetization of Tb_5Sn_4 measured in the ZFC and FC modes (a). The insets of (a) show the temperature dependence of inverse dc magnetic susceptibility of Tb_5Sn_4 measured in 100 Oe and 10 kOe applied fields. The magnetization in 100 Oe applied field of R_5Sn_4 (R = Dy, Ho, and Er) alloys (b). The inset of (b) shows the temperature dependence of inverse dc magnetic susceptibility.

17 wt.%. The R_5Sn_4 major phase in these alloys has the Sm_5Ge_4-type orthorhombic structure with space group *Pnma*. The lattice parameters and unit cell volumes of the R_5Sn_4 phases are listed in Table II. The decrease of the lattice parameters and unit cell volumes with increasing rare earth atomic number reflects the lanthanide contraction.

Magnetic measurements were carried out on all annealed samples. The $M(T)$ curve of Tb_5Sn_4 alloy measured in 100 Oe and 10 kOe applied fields in "zero-field-cooled" (ZFC) and "field-cooled" (FC) modes are shown in Fig. 1(a). The insets display the temperature dependence of the inverse dc magnetic susceptibility (H/M). The Curie temperature T_C, defined as the temperature at the maximum of $|dM/dT|$ vs T plot, is ~84 K. The positive paramagnetic Curie temperature (θ_p) obtained from the Curie Weiss fit and the magnetization isotherms shown in the inset of Fig. 2 indicate that the magnetic state of the Tb_5Sn_4 alloy is ferrimagnetic. A cusp in the low field $M(T)$ data and a peak in the high field data were observed at 54 K. Considering the amount of the major impurity phase ($Tb_{11}Sn_{10}$, 7.3 wt.%) and the large magnitude of the peak observed at 54 K with a 10 kOe field, it is unlikely that the cusp and peak are caused by the impurity phases. Similar to Tb_5Ge_4,[13] we assigned the cusp and peak observed at 54 K to a spin reorientation in Tb_5Sn_4. There is an

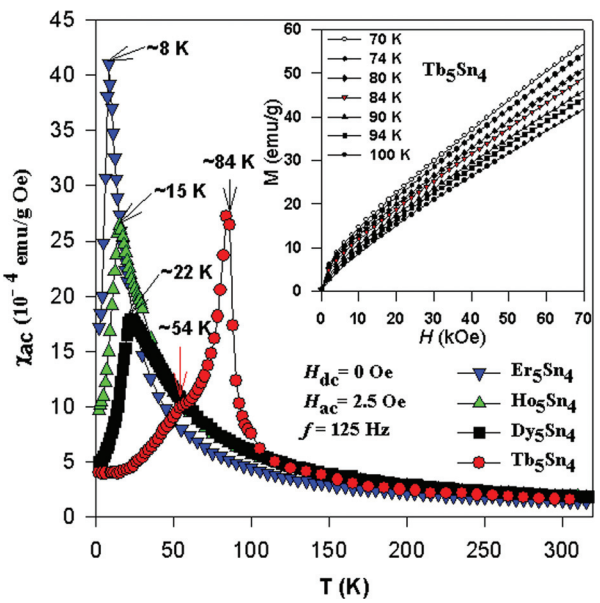

FIG. 2. (Color online) Temperature dependence of the ac magnetic susceptibility of R_5Sn_4 (R = Tb, Dy, Ho, and Er) alloys. The inset shows magnetization isotherms of Tb_5Sn_4 alloy with increasing magnetic field.

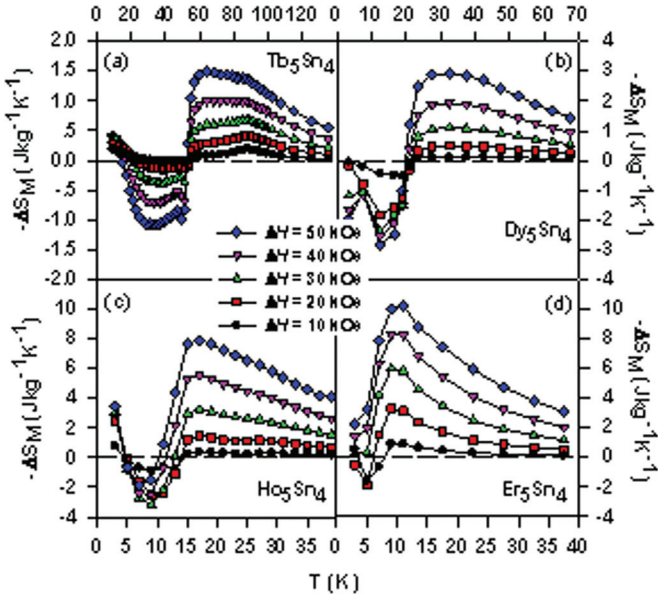

FIG. 3. (Color online) Temperature dependence of isothermal magnetic entropy changes ($-\Delta S_M$) of R_5Sn_4 (R = Tb, Dy, Ho, and Er) alloys for various magnetic field changes.

additional kink near 16 K [Fig. 1(a)], whose origin needs further investigation.

The temperature dependencies of dc magnetization measured with a 100 Oe field for the R_5Sn_4 (R = Dy, Ho, and Er) alloys are shown in Fig. 1(b). The $M(T)$ curves exhibit a typical antiferromagnetic behavior, which agrees with the negative θ_p values as shown in the inset of Fig. 1(b). The Néel temperatures are 22, 14, and 8 K for Dy_5Sn_4, Ho_5Sn_4, and Er_5Sn_4 alloys, respectively.

The temperature dependencies of the ac magnetic susceptibility for R_5Sn_4 (R = Tb, Dy, Ho, and Er) alloys are displayed in Fig. 2. For Tb_5Sn_4 alloy, a distinct anomaly (peak) is observed at T_C (~84 K), and a cusp near ~54 K indicates a spin-reorientation. The results are in good agreement with the temperature dependent dc magnetization measured with a 100 Oe applied field. The antiferromagnetic-paramagnetic phase transitions occur at about 22, 15, and 8 K for Dy_5Sn_4, Ho_5Sn_4, and Er_5Sn_4 alloys, respectively. The Néel points determined from the ac and dc magnetic susceptibility are in good agreement.

Figures 3(a)–3(d) show the ($-\Delta S_M$) ~T for different magnetic field changes for Tb_5Sn_4, Dy_5Sn_4, Ho_5Sn_4, and Er_5Sn_4, respectively. The $-\Delta S_M$ vs T plot of Tb_5Sn_4 alloy exhibits a negative plateau between 20 and 52 K. It changes sign and exhibits a positive plateau at higher temperatures (60 ~ 95 K). The sign change occurs in the vicinity of the spin re-orientation transition. Figs. 3(b)–3(d) indicate that the magnetic entropy changes of Dy_5Sn_4, Ho_5Sn_4, and Er_5Sn_4 show a similar negative to positive sign change behavior. Since the ($-\Delta S_M$) of an antiferromagnet is negative; while for a ferromagnet, it is positive.[14] The change of the sign of the $-\Delta S_M$ in our R_5Sn_4 alloys is likely due to a change of the magnetic structure between antiferromagnetically and ferromagnetically dominated states caused by the applied field. The maximum $-\Delta S_M$ values for these R_5Sn_4 alloys with R = Tb, Dy, Ho, and Er are 1.49, 2.92, 7.95, and 10.25 J/kg K, respectively, with a field change of 50 kOe.

We note that the Tb_5Sn_4 alloy exhibits thermal irreversibility with low applied field, spin reorientation, and ferrimagnetic behaviors, which are different from Dy_5Sn_4, Ho_5Sn_4, and Er_5Sn_4 alloys. Noticeable differences in the magnetic properties among R_5Ge_4 (R = Tb, Dy, Ho, and Er) were also observed. Such differences are not surprising given the differences of these rare earth ions. To understand underlying mechanism, detailed magnetic structure information on these alloys is needed.

In summary, 5:4, 11:10, and 5:3 phases coexist in the annealed R_5Sn_4 alloys with R = Tb, Dy, Ho, and Er. The major R_5Sn_4 phase in these alloys has the Sm_5Ge_4-type orthorhombic structure with space group *Pnma*. The content of 11:10 and 5:3 phases varies between 9 and 17 wt.%. Both the dc magnetization and ac susceptibility indicate that Tb_5Sn_4 alloy has a complex magnetic structure. The spin reorientation and ferrimagnetic-paramagnetic phase transitions occur near 54 and 84 K, respectively. For Dy_5Sn_4, Ho_5Sn_4, and Er_5Sn_4 alloys, the antiferromagnetic-paramagnetic phase transition occurs at about 22, 15, and 8 K respectively. The ($-\Delta S_M$) of all alloys change sign from negative to positive with increasing temperature, which could be attributed to the change of the magnetic state of the compound.

This work was performed at the Ames Laboratory under Contract No. DE-AC02-07CH11358. X.C. Zhong thanks the Guangdong Provincial Science & Technology Program (Grant No. 2007B010600043) and the Fundamental Research Funds for the Central Universities (Grant No. 2009ZM0291) for financial support.

[1] V. K. Pecharsky and K. A. Gschneidner, Jr., Phys. Rev. Lett. **78**, 4494 (1997).
[2] L. Morellon, C. Magen, P. A. Algarabel, M. R. Ibarra, and C. Ritter, Appl. Phys. Lett. **79**, 1318 (2001).
[3] V. V. Ivtchenko, V. K. Pecharsky, and K. A. Gschneidner, Jr., Adv. Cryog. Eng. Mater. **46**, 405 (2000).
[4] A. O. Pecharsky, K. A. Gschneidner, Jr., V. K. Pecharsky, D. L. Schlagel, and T. A. Lograsso, Phys. Rev. B **70**, 144419 (2004).
[5] D. H. Ryan, M. Elouneg-Jamróz, J. van Lierop, Z. Altounian, and H.B. Wang, Phys. Rev. Lett. **90**, 117202 (2003).
[6] V. K. Pecharsky and K. A. Gschneidner, Jr., Pure Appl. Chem. **79**, 1383 (2007).
[7] M. V. Bulanova, V. N. Eremenko, V. M. Petjukh, and V. R. Sidorko, J. Phase Equilib. **19**, 136 (1998).
[8] H. Okamoto, J. Phase Equilib. **16**, 197 (1995).
[9] V. T. Witusiewicz, V. R. Sidorko, and M. V. Bulanova, J. Alloys Compd. **248**, 233 (1997).
[10] V. K. Pecharsky and K. A. Gschneidner, Jr., J. Appl. Phys. **86**, 565 (1999).
[11] V. N. Eremenko, M. V. Bulanova, and P. S. Martsenyuk, Sov. Prog. Chem. **57**, 14 (1990). Calculated from LPF using POWD-12++.
[12] V. N. Eremenko, M. V. Bulanova, and P. S. Martsenyuk. J. Alloys Compds. **189**, 229 (1992). Calculated from LPF using POWD-12++.
[13] C. Ritter, L. Morellon, P. A. Algarabel, C. Magen, and M. R. Ibarra, Phys. Rev. B **65**, 094405 (2002).
[14] A. M. Tishin and Y. I. Spichkin, The Magnetocaloric Effect and Its Applications (Institute of Physics, Bristol, 2003).